analytical chemistry

Subscriber access provided by UNIV OF CAMBRIDGE

Article

Direct surface analysis coupled to high-resolution mass spectrometry reveals heterogeneous composition of the cuticle of Hibiscus trionum petals

Chiara Giorio, Edwige Moyroud, Beverley J. Glover, Paul C. Skelton, and Markus Kalberer

Anal. Chem., **Just Accepted Manuscript** • Publication Date (Web): 03 Sep 2015

Direct surface analysis coupled to high-resolution mass spectrometry reveals heterogeneous composition of the cuticle of *Hibiscus trionum* petals

Chiara Giorio[1*], Edwige Moyroud[2], Beverley J. Glover[2], Paul C. Skelton[1] and Markus Kalberer[1*]

[1] Department of Chemistry, University of Cambridge, Lensfield Road, Cambridge, CB2 1EW, United Kingdom; [2] Department of Plant Sciences, University of Cambridge, Downing Street, Cambridge, CB2 3EA, United Kingdom;

*corresponding authors: Phone: +44 1223 763615; +44 1223 336487. Fax: +44 (0) 1223 336362. E-mail: chiara.giorio@atm.ch.cam.ac.uk; markus.kalberer@atm.ch.cam.ac.uk

Abstract

Plant cuticle, the outermost layer covering the aerial parts of all plants including petals and leaves, can present a wide range of patterns, which, combined with cell shape, can generate unique physical, mechanical or optical properties. For example, arrays of regularly spaced nanoridges have been found on the dark (anthocyanin-rich) portion at the base of the petals of *Hibiscus trionum*. Those ridges act as a diffraction grating, producing an iridescent effect. As the surface of the distal white region of the petals is smooth and non-iridescent, a selective chemical characterisation of the surface of the petals on different portions (i.e. ridged vs. smooth) is needed to understand whether distinct cuticular patterns correlate with distinct chemical compositions of the cuticle. In the present study a rapid screening method has been developed for the direct surface analysis of *Hibiscus trionum* petals using liquid extraction surface analysis (LESA) coupled to high-resolution mass spectrometry. The optimised method was used to characterise a wide range of plant metabolites and cuticle monomers on the upper (adaxial) surface of the petals on both the white/smooth and anthocyanic/ridged regions, and on the lower (abaxial) surface, which is entirely smooth. The main components detected on the surface of the petals are low-molecular-weight organic acids, sugars and flavonoids. The ridged portion on the upper surface of the petal is enriched in long chain fatty acids which are constituents of the wax fraction of the cuticle. These compounds were not detected on the white/smooth region of the upper petal surface or on the smooth lower surface.

Keywords

LESA-MS, direct surface analysis, HRMS, cuticle, petal, *Hibiscus trionum*

Introduction

Plant cuticle is the outermost layer that covers the epidermis of the aerial organs of plants, including leaves and petals. The primary function of the plant cuticle is to limit water loss by evaporation and to regulate gas exchange, but it also contributes to normal organ development and it protects the plant against mechanical injury from the environment, attack from pathogens and damage caused by UV radiation.[1–3]

This lipophilic protective layer is synthesized by epidermal cells as a complex mixture of waxes embedded in a polymer of cutin. The chemical composition of the cuticle varies widely between plant species, organs and growth stages[4–7] but the main components are cutin, a polymer of oxygenated C16 and C18 fatty acids (mainly hydroxy fatty acids) cross-linked by ester bonds, and waxes. These can be either epicuticular waxes (directly exposed on the surface) and/or intracuticular waxes (embedded in the cutin layer), and are mainly mixtures of C20-C40 n-alcohols, n-aldehydes, n-alkanes and n-carboxylic acids, also named very long chain fatty acids (VLCFAs).[1] Phenolic compounds and carbohydrates have also been reported as minor structural components of the cuticle.[3] Another cuticle component is cutan, a polymer made of polyunsaturated fatty acids mainly linked to each other through ether bonds, which is present either as an alternative to or in combination with cutin.[1] In addition, low-molecular-weight compounds, either exogenous (e.g. adjuvants or pesticides) or endogenous (e.g. phenolic compounds and flavonoids), can be found in the typical cavities present in amorphous and cross-linked polymers like cutin.[1]

Characteristic patterning of the cuticle on top of epidermal cells, as micro- or nanostructures on the surface of petals, leaves and fruits, can give rise to a wide range of physical, mechanical and optical properties.[8] For instance, nanoscale patterning of the cuticle has been shown to interfere with the ability of insects to adhere to a surface,[9,10] to provide a high adhesive force with water (known as the 'petal effect') and superhydrophobicity (such as the self-cleaning 'lotus effect') [9,11,12] and to generate optical effects.[13,14] In the latter case, arrays of regularly spaced nanoridges have been found on the flat epidermis of *Hibiscus trionum* (also known as Venice mallow or flower of an hour) and many species of tulips, where they act as diffraction gratings, creating structural colours that vary with the observation angle, a phenomenon known as iridescence.[8,14,15] In *Hibiscus trionum,* the diffraction grating is restricted to the basal purple (anthocyanin-rich) half of the petal on the upper surface (Figure 1), as only those epidermal cells display the flat elongated shape and characteristic regularly spaced nanoridges necessary to produce iridescence (Figure 2a). In the upper white half of the petal the epidermal cells do not produce any iridescence: those cells are radically

different, with a conical shape and a smooth cuticle (Figure 2b). The cuticle pattern in *Hibiscus trionum* is easy to distinguish by eye because ridges overlie the anthocyanic portion and not the white portion (Figure 1a), but the pigment is present as intracellular compound and not in the cuticle. The biological function of diffraction-grating-like structures on petal surfaces remains unclear but they may facilitate pollination, as bumblebees can use iridescence to detect flowers.[15] Thus, nanoscale patterns on the plant surface play a significant role in the interactions of the plant with the biotic and abiotic environment, but the physical processes and/or chemical composition of the materials involved in the formation of these structures are largely unknown.[8] Indeed, the constituents of the cuticle itself could play a key role in conditioning the type of nanopattern produced. Thus, a detailed understanding of the chemical composition of the cuticle may help us to understand how different patterns arise in different regions of the *Hibiscus trionum* petal.

Characterisation of plant cuticles has been largely done by extracting and depolymerising bulk samples of cutin followed by NMR, FTIR and mass spectrometry analyses.[2,3,16–22] These methods generally involve time-consuming and cumbersome sample preparation. In order to obtain reliable estimates of cutin composition, particular precautions need to be taken throughout the entire workup, e.g. use of antioxidants during solvent extraction to avoid peroxidation of lipids, rigid anhydrous conditions during derivatisation, avoiding contamination throughout each individual sample preparation step (extraction, depolymerisation, separation, derivatisation). The most commonly used methods consists of bulk extraction followed by a depolymerisation step (e.g. acid or base digestion) to break-down the biomacromolecules into their constituent monomers which are then derivatised to methyl or trimethylsilyl esters prior to analysis with GC[18,19] or GC-MS.[2,18,23] More recently, a novel method was described using nanoelectrospray ionisation (nanoESI) mass spectrometry to characterise cuticle components.[24] Differences of the cuticle composition observed in various studies might have been caused in part by the bulk extraction procedures[2] and thus surface selective extraction methods would be highly advantageous.

A more selective characterisation of plant cuticle on upper and lower surfaces of leaves can be done by mechanically stripping off and/or extracting in chloroform the respective sides. The resulting wax solution can then be derivatised and analysed using the methods described above.[17] However, stripping off the epidermis and its cuticle is not always possible, depending on the plant species studied, as some tissues, such as petals, are much more fragile than others and this does not completely circumvent the problem of contamination from other tissues. More recently, direct surface analysis using mass spectrometry has been applied to

characterise biological tissues using matrix-free laser desorption/ionisation[25–27] and desorption electrospray ionisation (DESI)[27–29] mass spectrometry. DESI-MS has been successfully applied for direct imaging of plant metabolites in leaves and petals of *Hypericum perforatum*.[28,29]

Liquid extraction surface analysis (LESA) is a newly developed technique for surface specific organic analysis.[30–32] In LESA, a conductive pipette tip is positioned above the surface to be sampled and a small amount of extraction solvent, usually a few μL, is dispensed without breaking the liquid junction between the pipette tip and the surface of the sample. The diameter of the extraction spot is generally slightly larger than the 1-mm diameter of the pipette tip. After that, the solution containing the dissolved sample is aspirated back into the tip and sprayed through a nanoESI nozzle.[31,32] In contrast to DESI, LESA allows optimisation of the time in which the solvent droplet is in contact with the surface under analysis, giving greater control over the extraction step and higher extraction efficiency. LESA has already been applied successfully to analysis of biological samples,[33,34] food,[35] aerosol[36] and pharmacokinetic studies[37,38] but it has not previously been used to compare different areas of the surface of a single plant tissue.

In this study, a method utilising LESA coupled to high-resolution mass spectrometry (HRMS) has been developed and optimized for spatially resolved, rapid screening of plant metabolites, cutin and wax monomers on the surface of petals of *Hibiscus trionum*. The approach adopted has proved to be useful to characterise compositional differences between the anthocyanic/ridged and white/smooth portions of the petals on both the upper surface of the petals and the lower surface. To the authors knowledge, this is the first application of LESA-MS to characterize different areas of a single plant tissue to investigate links between composition and structure on plant surfaces.

Materials and Methods

Plant growth conditions

Petals of *Hibiscus trionum* L. used in this studied were harvested from plants grown in glasshouse condition in Levington's (UK) compost from seeds obtained from Chiltern seeds (http://www.chilternseeds.co.uk). Supplemental lightning was provided through Osram 400W high-pressure sodium lamps (Osram, München, Germany) on a 16h:8h, light:dark

photoperiod. Fully open flower were collected between 8am and 10am when the plants are in full bloom and kept at 4°C until analysis (typically less than 3 days).

LESA-MS

Sample preparation

Petals of *Hibiscus trionum* were detached from the flowers using tweezers and then cleaned with a dry white nylon brush followed by a gentle N_2 flow. Cleaned petals, with either the upper or lower surface facing upward, were then placed on a movable LESA sample stage covered with cleaned aluminium foil. Particular care is necessary to handle the petals and place them onto the movable sample plate as the petals are curved and easily break during operations.

Instrumental analysis

LESA-MS analysis was done on the anthocyanic/ridged and white/smooth portions of the petals on the upper surface and on the anthocyanic/smooth and white/smooth portions of the petals on the lower surface (Figure 1b) using two different solvent mixtures (details on reagents and chemicals used are reported in the supporting information, section S1.1): a more polar acetonitrile-water (90:10) mixture, called polar mixture hereafter, and a more nonpolar chloroform-acetonitrile-water (49:49:2) mixture,[28] called nonpolar mixture hereafter. In order to increase spray stability and ionisation efficiency 0.1% formic acid was added to the water used in both solvent mixtures.[39,40]

Three μL of solvent were deposited at a height of 1.4 mm from the sample plate at the maximum dispensation rate (60 μL/min). The liquid junction was maintained for 30 s for the nonpolar mixture and for 45 s for the polar mixture. Longer contact times led to breakdown of the liquid junction due to solvent evaporation. The droplets containing the dissolved analytes were then aspirated at a height of 1.2 mm from the sample plate at the maximum aspiration rate (60 μL/min) and infused in a chip-based nanoESI source (Triversa NanoMate Advion, Ithaca, USA). Blanks were analysed by repeating the same procedure on the clean aluminium foil, with a dispensation height of 1.2 mm and aspiration height of 1.0 mm from the surface.

A high-resolution mass spectrometer (LTQ Velos Orbitrap, Thermo Scientific, Bremen, Germany) with a resolution of 100 000 at m/z 400 and a typical mass accuracy within ±2 ppm was used to analyze the organic compounds present in the samples following extraction by LESA. Samples were sprayed at a gas (N_2) pressure of 0.30 psi at 1.8 kV in positive ionisation mode and 0.80 psi at -1.4 kV in negative ionisation mode with a transfer capillary temperature of 210ºC. Data were acquired using an automated acquisition method to measure the full scan in m/z range 80-600 and 150-1000 and auto MS/MS analysis on the five most intense peaks with a collision induced dissociation (CID) energy of 30 (normalised collision energy). For each droplet a minimum of 30 scan routines were acquired (ca. 3 minutes of acquisition). The instrument was calibrated routinely to within ± 2 ppm accuracy using a Pierce™ LTQ Velos ESI Positive Ion Calibration Solution and a Pierce™ ESI Negative Ion Calibration Solution (Thermo Scientific). Details of the data treatment are reported in the supporting information (section S1.2).

Results and discussion

Optimisation of the analytical method in LESA-MS

Selection of extraction solvent

Three different solvent mixtures, with different polarities, were tested initially for analysis of the cuticle of *Hibiscus trionum* petals: methanol-water (90:10), acetonitrile-water (90:10) and chloroform-acetonitrile-water (49:49:2) similarly to Li *et al*.[29] and Hemalatha and Pradeep.[28] The three mixtures were compared in terms of spray stability and efficiency of extraction for which the total ion current (TIC) in the MS was used as indicator. Concerning the upper surface of the petals, the two polar mixtures (methanol-water and acetonitrile-water) gave comparable results for analysis of the white/smooth portion of the petal with higher spray stability (RSD ~5%) and TIC compared with the nonpolar mixture (chloroform-acetonitrile-water). The acetonitrile-water mixture resulted in higher TIC for the anthocyanic/ridged portion of the petal compared to the methanol-water mixture. The nonpolar mixture yielded more stable (RSD ~5%) and higher TIC for the anthocyanic/ridged portion of the petal and the lower surface of the petal compared to the two polar mixtures. Although the overall number of peaks detected was not significantly different with the three extraction mixtures, to assure a most comprehensive analysis, all portions of the petals were analysed with both one

of the polar (acetonitrile-water) and the nonpolar (chloroform-acetonitrile-water) solvent mixtures, whereas the methanol-water mixture was not used in the results discussed below.

Optimisation of extraction parameters

Extraction volumes ranging between 1-3 μL were tested. An extraction volume of 1 μL allowed us to acquire data for only about 1 minute, corresponding to only a few MS scan routines. A partial evaporation of the solvent during the extraction step, which reduces the amount of sample available for analysis, was the main reason for the limited acquisition time. Three μL of solvent were sufficient to acquire mass spectra for up to 5 minutes.

Contact time of the liquid junction with the petal surface was also tested between 30 and 90 seconds with a single deposition/aspiration cycle or divided into two deposition/aspiration cycles. Using the acetonitrile-water mixture, the TIC increased about 10 times with a contact time of 60 seconds compared with 30 seconds indicating that the extraction efficiency had increased. Longer contact times are less effective (the TIC did not increased significantly compared with a contact time of 60 seconds) and lead to breakdown of the liquid junction. For the nonpolar mixture (chloroform-acetonitrile-water), the longest contact time before breakdown of the liquid junction occurs was 45 seconds because of the higher volatility of chloroform.

Previous studies showed that repeatedly depositing and aspirating solvent onto a single extraction spot aids mixing of the extracted sample into the droplet within a short contact time of typically 1-5 s.[38,41] However, this leads to sample loss through each deposition/aspiration cycle as a small amount of solvent is lost to the surface each time the sample is aspirated. A single but longer deposition/aspiration cycle reduces sample loss while increasing the time for sample extraction and still allowing mixing through diffusion due to the small extraction volume.[36,42]

Dispensation and aspiration height were adjusted according to the volume of the droplet in order to maintain the liquid junction during the extraction time. Optimal dispensation and aspiration heights were 1.4 mm and 1.2 mm, respectively, from the sample plate for all samples and 1.2 mm and 1.0 mm, respectively, for blanks (pre-washed aluminium foil). Dispensation and aspiration rates did not have a significant effect on extraction efficiency and they were kept at the maximum rate (60 μL/min).

Results of LESA-MS analysis

Repeatability between different samples

Repeatability has been evaluated in terms of peak detection as in direct infusion ESI-MS analysis the intensity of the peaks cannot be directly related to concentration of the compounds being measured.

In all 4 analysed parts of the petals, i.e. anthocyanic and white portions on both the upper and lower surfaces, about 50% of all peaks measured in a given portion were found to be present in at least two extraction spots among 6-10 replicates from 2-4 petals, each of them from different flowers collected from different plants (Table S-1, Figures S-1 and S-2). Only about 13-36% of all peaks were found in at least three replicates. The repeatability did not increase significantly when considering only analyses done on the same petal (intrapetal variability). Part of the variability may arise from the strongly conservative approach used to remove the instrumental noise (~10 S/N cut off).[43] This very conservative approach has been used in order to avoid the inclusion of background noise in the final list of molecular formulas.

The relatively low repeatability of this direct surface extraction contrasts with a much higher repeatability of methanolic extracts of the petals for which about 80% of peaks were found in at least 3 instrumental repeats out of 3, which is similar to previous studies using direct infusion.[43,44] The high variability in direct surface analysis could be attributed to inhomogeneity in the amount and distribution of plant metabolites and cutin/wax monomers on the surface of the petals. A previous study using DESI-MS also observed an uneven distribution of plant metabolites on the surface of leaves and petals of *Hypericum perforatum*.[29] For all these reasons, the sum of all peaks detected in the different replicate MS measurements in the different portion of the petals are considered further for the discussion below.

Main components

The compounds with highest signal intensities in the mass spectra, tentatively identified using their accurate mass and MS/MS spectra, in all regions of the petals (on both upper and lower surfaces) are mainly plant metabolites which can be divided into three main classes: (i) low-molecular-weight organic acids (LMWOAs), (ii) sugars and (iii) flavonoids (Table 1).

The main compound in the first class is malic acid, which is one of the most intense peaks in every mass spectra recorded in negative ionisation. Other identified compounds are ascorbic

and dehydroascorbic acids, gallic acid, citric acid, quinic acid and gluconic acid, all previously detected in other species of *Hibiscus* plants.[45–51]

Among sugars, peaks of monosaccharides and disaccharides were detected in all samples in both positive and negative ionisation. These are present as protonated and deprotonated molecular ions (in positive and negative ionisation, respectively) but also as sodium and potassium adducts in positive ionisation and as chloride adducts in negative ionisation. The peaks of the chloride adducts are particularly intense when the nonpolar solvent mixture is used, which can be attributed to the presence of chloroform. Chlorinated solvents may produce chloride anions by dissociative electron capture in corona discharge conditions or electrochemical reduction at the ESI capillary.[52] Alternatively, chloride adducts could also be formed from chloride salts present in the tissue.

The main compounds in the flavonoids class are gossypetin and gossypin, which has been previously identified in *Hibiscus sabdariffa* and *Hibiscus vitifolius*.[53–55]

Additionally, glutamine has been identified in all samples, together with malic acid hexoside and palmitic acid. The latter is a known precursor of epicuticular wax monomers.[56]

A series of sulfur containing compounds was identified in all samples with molecular formulas consistent with C15-C18 benzenesulfonates and a compound with the formula $C_{15}H_{28}O_6S$; however we were unable to further elucidate their structure or their biological significance (if any).

In addition, pigments present mainly as intracellular compounds were analysed by bulk extraction of the petals followed by analysis in LC-UV/Vis-MS. Experimental details and results of these chromatographic analyses are reported in the supporting information (sections S1.3 and S2.1).

Comparison between white/smooth and anthocyanic/ridged portions on the upper surface of the petals

The nonpolar extraction mixture resulted in better extraction efficiency and thus higher TIC and more stable currents for the anthocyanic/ridged portion of the petal while the polar mixture resulted in higher TIC and more stable spray current for the white/smooth portion of the petal (see also section 3.1.1). This suggests that the anthocyanic/ridged and white/smooth portions of the petals may have a different overall surface composition with more nonpolar compounds on the anthocyanic/ridged region.

The molecular characterisation of the surfaces in the two regions of the petals confirms this hypothesis (Table S-2, Figure 2c and 2d). The average (non-weighted for intensity of peaks) carbon oxidation state ($\overline{OS}c$), a metric to describe the degree of oxidation of organic compounds,[57] for the anthocyanic/ridged region was -0.51 ± 0.31 (n=8), which is statistically different (*t*-test, $p < 0.001$) to that of the white/smooth region which was 0.11 ± 0.15 (n=10). The majority of compounds present exclusively in the anthocyanic/ridged portion are distributed between two regions of the van Krevelen diagram[58] (Figure 3a), the region of lipids[58] (red square in Figure 3a) and the region of condensed (unsaturated) hydrocarbons[58] (blue square in Figure 3a). In contrast, the vast majority of compounds only present in the white/smooth region are in the area with O/C > 0.6 (green square in Figure 3a). The white/smooth region is more abundant in short chain dicarboxylic acids and hydroxydicarboxylic acids explaining their high O/C.

More detailed information can be extracted by Kendrick mass defect plots, which help to identify homologous series of compounds having the same constitution of heteroatoms, same number of rings/double bonds but different chain length (number of $–CH_2$ groups).[59]

As shown by the Kendrick mass defect plot (Figure 4a and Figure S-1), the main series of compounds present exclusively in the anthocyanic/ridged portion of the petals are characterised by long chain saturated fatty acids, hydroxy fatty acids, dihydroxy fatty acids, and monounsaturated hydroxy fatty acids, which are all known components of epi- and intracuticular waxes (Table S-2). In addition, series of long chain highly unsaturated compounds (Figure 4a) and $\overline{OS}c < -0.8$ (Figure 4b) are also present exclusively in the anthocyanic/ridged portion of the petal and may be also associated with cuticular waxes. These results are supported by TEM images which have shown that the cuticle of the anthocyanic/ridged portion of the petal is topped by a very electron-dense layer (see Figure 1e in Vignolini *et al.*[14]). The chemical nature of electron-dense layers in the cuticle is often obscure but it could be associated with a denser cutin polymer or it could reflect the wax-rich nature of the cuticle in this portion of the petal, as cuticular waxes are preferentially deposited in the outer fractions of the cuticle (see reviews by Riederer and Friedmann,[60] and Schreiber[61]). The presence of numerous cuticular waxes on or near the surface also explains the increased extraction efficiency when the nonpolar solvent mixture is used.

Comparison between upper and lower surface of the petals

To examine if the presence of a wax-rich cuticle correlates with the presence of a ridged nanopattern, we analysed the back (lower surface) of the petal. Here, the cells are flat (like the cells in the anthocyanic portion on the upper side of the petal) but with a smooth cuticle (similar to the cuticle in the white portion on the upper surface of the petal).

The results of the LESA-MS analysis showed that the anthocyanic/smooth and white/smooth portions on the lower surface of the petals are not characterised by a distinct cuticle compositional difference (Figure S-2), as opposed to what was observed for the upper surface of the petals (Figure S-1).

On the lower surface of the petal, the nonpolar solvent mixture gave higher TIC and more stable spray currents than the polar solvent mixture for both the white and anthocyanic portions. This suggests that the lower surface is more hydrophobic than the white region on the upper surface.

The average $\overline{OS}c$ for the lower surface is -0.17 ± 0.16 (Table S-3) and it is statistically the same in the white and anthocyanic portions of the petal (*t*-test, $p > 0.025$). The $\overline{OS}c$ of the lower surface is lower than in the white/smooth portion on the upper surface but higher than in the anthocyanic/ridged region of the upper surface. As shown in Figure 3a, a large cluster of compounds is present exclusively in the lower surface of the petal with $O/C < 0.6$ and H/C between 1 and 2 (black circle in Figure 3a). A molecular characterisation shows that on the lower surface longer chain less oxidized compounds are more abundant than in the white/smooth portion on the upper surface (green circles in Figure S-2a and S-2b). However, they are shorter and more oxidised than in the anthocyanic/ridged portion on the upper surface (purple circle in Figure S-1a). These compounds are mainly C20-C30 polyunsaturated compounds, which could be tentatively assigned to polyunsaturated fatty acids (black circle in Figure 3b). In several species such as *Arabidopsis thaliana, Petunia hybrida, Cistus albidus* and *Cosmos bipinnatus*, it has been shown that petal cuticles are characterised by shorter chain length waxes than those found in the vegetative organs of the same species.[22,62–65] Interestingly, our analysis suggests that wax chain length could also differ between the two sides of the same organ.

Conclusions

We developed a direct surface extraction MS method for selective and spatially resolved characterisation of the surface of plant organs. With the optimised rapid screening method a wide range of plant metabolites were detected together with cutin/wax monomers on both the upper and lower surface of the petals. Conventional methods of analysis of the cuticle are more laborious and are not often suitable to selectively characterise different portions of a single tissue with enough accuracy.

Distinct compositional differences between the different portions of the petals of *Hibiscus trionum* could be identified. On the upper surface of the petals the anthocyanic/ridged portion is more hydrophobic, with an average $\overline{OS}c$ of -0.51 ± 0.31, than the white/smooth portion ($\overline{OS}c$ 0.11±0.15). The anthocyanic/ridged portion of the petal is enriched in VLCFAs, common constituents of waxes, which seems to be the main compositional difference between the anthocyanic/ridged and white/smooth portions of the petals in our LESA-MS analyses. The lower surface of the petals, which is entirely smooth, presents an intermediate hydrophobicity ($\overline{OS}c$ -0.17 ± 0.16), it is enriched in C20-C30 polyunsaturated compounds and it is not characterised by a distinct compositional difference between the anthocyanic and white portions. Our results are consistent with previous studies which showed that the composition of the plant cuticle is indeed chemically and morphologically variable not only between species or organs but can also vary between different portions of the same organ as different specialized cells can produce and assemble distinct cuticular compounds (see reviews by Nawrath,[4] Jeffree,[5] Stark and Tian,[6] Jetter *et al.*[7] and references therein). Interestingly, the presence of VLCFAs correlates with the presence of ridges, thus it is possible that the chemical composition of the cuticle directly impacts the type of nanopattern produced. Further experiments are now necessary to test whether the unique nature of the cuticle in the anthocyanic/ridged region of the petal contributes directly to the formation of the diffraction grating and could explain why nanoridges develop on this portion of the petal only.

Supporting information

Additional experimental details and results including 3 tables and 4 figures.

Acknowledgements

The authors thank Matthew Dorling for excellent plant care, other members of the Glover lab for helpful discussions, Nathan Pitt (Photography and Reprographics, Dept. Chemistry, University of Cambridge) for help with TOC image and support by the ERC grant 279405.

References

(1) Dominguez, E.; Heredia-Guerrero, J. A.; Heredia, A. The biophysical design of plant cuticles: An overview. *New Phytologist*, 2011, *189*, 938–949.

(2) Mendez-Millan, M.; Dignac, M.-F.; Rumpel, C.; Derenne, S. *Org. Geochem.* **2010**, *41*, 187–191.

(3) Bonaventure, G.; Beisson, F.; Ohlrogge, J.; Pollard, M. *Plant J.* **2004**, *40*, 920–930.

(4) Nawrath, C. *Curr. Opin. Plant Biol.* **2006**, *9*, 281–287.

(5) Jeffree, C. E. In *Annual Plant Reviews Volume 23: Biology of the Plant Cuticle*; Riederer, M., Müller, C., Eds.; Blackwell Publishing Ltd: Oxford, UK, 2006; pp 11–125.

(6) Stark, R. E.; Tian, S. In *Annual Plant Reviews Volume 23: Biology of the Plant Cuticle*; Riederer, M., Müller, C., Eds.; Blackwell Publishing Ltd: Oxford, UK, 2006; pp 126–144.

(7) Jetter, R.; Kunst, L.; Samuels, A. L. In *Annual Plant Reviews Volume 23: Biology of the Plant Cuticle*; Riederer, M., Müller, C., Eds.; Blackwell Publishing Ltd: Oxford, UK, 2006; pp 145–181.

(8) Antoniou Kourounioti, R. L.; Band, L. R.; Fozard, J. A.; Hampstead, A.; Lovrics, A.; Moyroud, E.; Vignolini, S.; King, J. R.; Jensen, O. E.; Glover, B. J. *J. R. Soc. Interface* **2013**, *10*, 20120847.

(9) Prum, B.; Seidel, R.; Bohn, H. F.; Speck, T. *J. R. Soc. Interface* **2012**, *9*, 127–135.

(10) Poppinga, S.; Koch, K.; Bohn, H. F.; Barthlott, W. *Funct. Plant Biol.* **2010**, *37*, 952.

(11) Barthlott, W.; Neinhuis, C. *Planta* **1997**, *202*, 1–8.

(12) Feng, L.; Zhang, Y.; Xi, J.; Zhu, Y.; Wang, N.; Xia, F.; Jiang, L. *Langmuir* **2008**, *24*, 4114–4119.

(13) Whitney, H. M.; Kolle, M.; Andrew, P.; Chittka, L.; Steiner, U.; Glover, B. J. *Science* **2009**, *323*, 130–133.

(14) Vignolini, S.; Moyroud, E.; Hingant, T.; Banks, H.; Rudall, P. J.; Steiner, U.; Glover, B. J. *New Phytol.* **2015**, *205*, 97–101.

(15) Vignolini, S.; Moyroud, E.; Glover, B. J.; Steiner, U. *J. R. Soc. Interface* **2013**, *10*, 20130394.

(16) Deas, A. H. B.; Baker, E. A.; Holloway, P. J. *Phytochemistry* **1974**, *13*, 1901–1905.

(17) Ji, X.; Jetter, R. *Phytochemistry* **2008**, *69*, 1197–1207.

(18) Liu, K.-S. *J. Am. Oil Chem. Soc.* **1994**, *71*, 1179–1187.

(19) Riederer, M.; Schönherr, J. *J. Chromatogr. A* **1986**, *360*, 151–161.

(20) Tsubaki, S.; Sakumoto, S.; Uemura, N.; Azuma, J. *Food Chem.* **2013**, *138*, 286–290.

(21) Van Maarseveen, C.; Jetter, R. *Phytochemistry* **2009**, *70*, 899–906.

(22) Buschhaus, C.; Peng, C.; Jetter, R. *Phytochemistry* **2013**, *91*, 249–256.

(23) Eder, K. *J. Chromatogr. B. Biomed. Appl.* **1995**, *671*, 113–131.

(24) Iven, T.; Herrfurth, C.; Hornung, E.; Heilmann, M.; Hofvander, P.; Stymne, S.; Zhu, L.-H.; Feussner, I. *Plant Methods* **2013**, *9*, 24.

(25) Hölscher, D.; Shroff, R.; Knop, K.; Gottschaldt, M.; Crecelius, A.; Schneider, B.; Heckel, D. G.; Schubert, U. S.; Svatoš, A. *Plant J.* **2009**, *60*, 907–918.

(26) Vidová, V.; Novák, P.; Strohalm, M.; Pól, J.; Havlíček, V.; Volný, M. *Anal. Chem.* **2010**, *82*, 4994–4997.

(27) Nemes, P.; Vertes, A. *Trends Anal. Chem.* **2012**, *34*, 22–34.

(28) Hemalatha, R. G.; Pradeep, T. *J. Agric. Food Chem.* **2013**, *61*, 7477–7487.

(29) Li, B.; Hansen, S. H.; Janfelt, C. *Int. J. Mass Spectrom.* **2013**, *348*, 15–22.

(30) Ellis, S. R.; Brown, S. H.; In Het Panhuis, M.; Blanksby, S. J.; Mitchell, T. W. *Prog. Lipid Res.* **2013**, *52*, 329–353.

(31) Kertesz, V.; Van Berkel, G. J. *Rapid Commun. Mass Spectrom.* **2014**, *28*, 1553–1560.

(32) Kertesz, V.; Van Berkel, G. J. *J. mass Spectrom.* **2010**, *45*, 252–260.

(33) Sarsby, J.; Martin, N. J.; Lalor, P. F.; Bunch, J.; Cooper, H. J. *J. Am. Soc. Mass Spectrom.* **2014**, *25*, 1953–1961.

(34) Porta, T.; Varesio, E.; Hopfgartner, G. *Anal. Chem.* **2013**, *85*, 11771–11779.

(35) Montowska, M.; Alexander, M. R.; Tucker, G. A.; Barrett, D. A. *Anal. Chem.* **2014**, *86*, 10257–10265.

(36) Fuller, S. J.; Zhao, Y.; Cliff, S. S.; Wexler, A. S.; Kalberer, M. *Anal. Chem.* **2012**, *84*, 9858–9864.

(37) Swales, J. G.; Tucker, J. W.; Strittmatter, N.; Nilsson, A.; Cobice, D.; Clench, M. R.; Mackay, C. L.; Andren, P. E.; Takáts, Z.; Webborn, P. J. H.; Goodwin, R. J. A. *Anal. Chem.* **2014**, *86*, 8473–8480.

(38) Eikel, D.; Vavrek, M.; Smith, S.; Bason, C.; Yeh, S.; Korfmacher, W. a.; Henion, J. D. *Rapid Commun. Mass Spectrom.* **2011**, *25*, 3587–3596.

(39) Hua, Y.; Jenke, D. *J. Chromatogr. Sci.* **2012**, *50*, 213–227.

(40) Wu, Z.; Gao, W.; Phelps, M. A.; Wu, D.; Miller, D. D.; Dalton, J. T. *Anal. Chem.* **2004**, *76*, 839–847.

(41) Paine, M. R. L.; Barker, P. J.; Maclauglin, S. A.; Mitchell, T. W.; Blanksby, S. J. *Rapid Commun. Mass Spectrom.* **2012**, *26*, 412–418.

(42) Walworth, M. J.; ElNaggar, M. S.; Stankovich, J. J.; Witkowski, C.; Norris, J. L.; Van Berkel, G. J. *Rapid Commun. Mass Spectrom.* **2011**, *25*, 2389–2396.

(43) Sleighter, R. L.; Chen, H.; Wozniak, A. S.; Willoughby, A. S.; Caricasole, P.; Hatcher, P. G. *Anal. Chem.* **2012**, *84*, 9184–9191.

(44) Kourtchev, I.; Doussin, J.-F.; Giorio, C.; Mahon, B.; Wilson, E. M.; Maurin, N.; Pangui, E.; Venables, D. S.; Wenger, J. C.; Kalberer, M. *Atmos. Chem. Phys. Discuss.* **2015**, *15*, 5359–5389.

(45) Wong, P.-K.; Yusof, S.; Ghazali, H. M.; Man, Y. B. C. *Nutr. Food Sci.* **2002**, *32*, 68–73.

(46) Ali, B. H.; Al Wabel, N.; Blunden, G. *Phyther. Res.* **2005**, *19*, 369–375.

(47) Philip, D. *Phys. E Low-Dimensional Syst. Nanostructures* **2010**, *42*, 1417–1424.

(48) Nnam, N.; Onyeke, N. *Plant Foods Hum. Nutr.* **2003**, *58*, 1–7.

(49) Mohd-Esa, N.; Hern, F. S.; Ismail, A.; Yee, C. L. *Food Chem.* **2010**, *122*, 1055–1060.

(50) Lachance, M.-A.; Bowles, J. M.; Starmer, W. T.; Barker, J. S. F. *Can. J. Microbiol.* **1999**, *45*, 172–177.

(51) Ramirez-Rodrigues, M. M.; Plaza, M. L.; Azeredo, A.; Balaban, M. O.; Marshall, M. R. *J. Food Sci.* **2011**, *76*, 429–435.

(52) Zhu, J.; Cole, R. B. *J. Am. Soc. Mass Spectrom.* **2000**, *11*, 932–941.

(53) Chandrashekhar, V.; Ganapaty, S.; Ramkishan, A.; Narsu, Ml. *Indian J. Pharmacol.* **2013**, *45*, 575.

(54) Braunberger, C.; Zehl, M.; Conrad, J.; Fischer, S.; Adhami, H. R.; Beifuss, U.; Krenn, L. *J. Chromatogr. B Anal. Technol. Biomed. Life Sci.* **2013**, *932*, 111–116.

(55) Al-Hashimi, A. G. *African J. Food Sci.* **2012**, *6*, 506–511.

(56) Wellesen, K.; Durst, F.; Pinot, F.; Benveniste, I.; Nettesheim, K.; Wisman, E.; Steiner-Lange, S.; Saedler, H.; Yephremov, A. *Proc. Natl. Acad. Sci. U. S. A.* **2001**, *98*, 9694–9699.

(57) Kroll, J. H.; Donahue, N. M.; Jimenez, J. L.; Kessler, S. H.; Canagaratna, M. R.; Wilson, K. R.; Altieri, K. E.; Mazzoleni, L. R.; Wozniak, A. S.; Bluhm, H.; Mysak, E. R.; Smith, J. D.; Kolb, C. E.; Worsnop, D. R. *Nat. Chem.* **2011**, *3*, 133–139.

(58) Kim, S.; Kramer, R. W.; Hatcher, P. G. *Anal. Chem.* **2003**, *75*, 5336–5344.

(59) Hughey, C. A.; Hendrickson, C. L.; Rodgers, R. P.; Marshall, A. G.; Qian, K. *Anal. Chem.* **2001**, *73*, 4676–4681.

(60) Riederer, M.; Friedmann, A. In *Annual Plant Reviews Volume 23: Biology of the Plant Cuticle*; Riederer, M., Müller, C., Eds.; Blackwell Publishing Ltd: Oxford, UK, 2006; pp 250–279.

(61) Schreiber, L. *Trends Plant Sci.* **2010**, *15*, 546–553.

(62) Hennig, S.; Guelz, G.; Hangst, K. *Zeitschrift für Naturforsch. C.* **1988**, *43*, 806–812.

(63) Jenks, M. a.; Tuttle, H. a.; Eigenbrode, S. D.; Feldmann, K. a. *Plant Physiol.* **1995**, *108*, 369–377.

(64) King, A.; Nam, J. W.; Han, J.; Hilliard, J.; Jaworski, J. G. *Planta* **2007**, *226*, 381–394.

(65) Shi, J. X.; Malitsky, S.; de Oliveira, S.; Branigan, C.; Franke, R. B.; Schreiber, L.; Aharoni, A. *PLoS Genet.* **2011**, *7*.

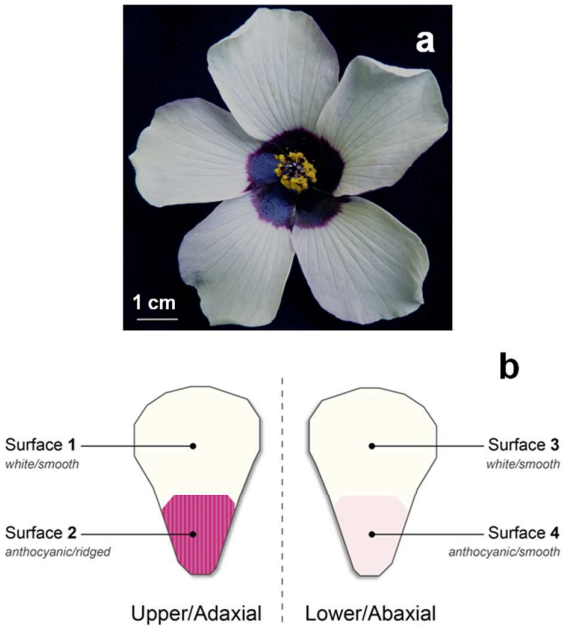

Figure 1. Picture of a flower of *Hibiscus trionum* (a) and diagram showing the different portions of the petals analysed in this study (b).

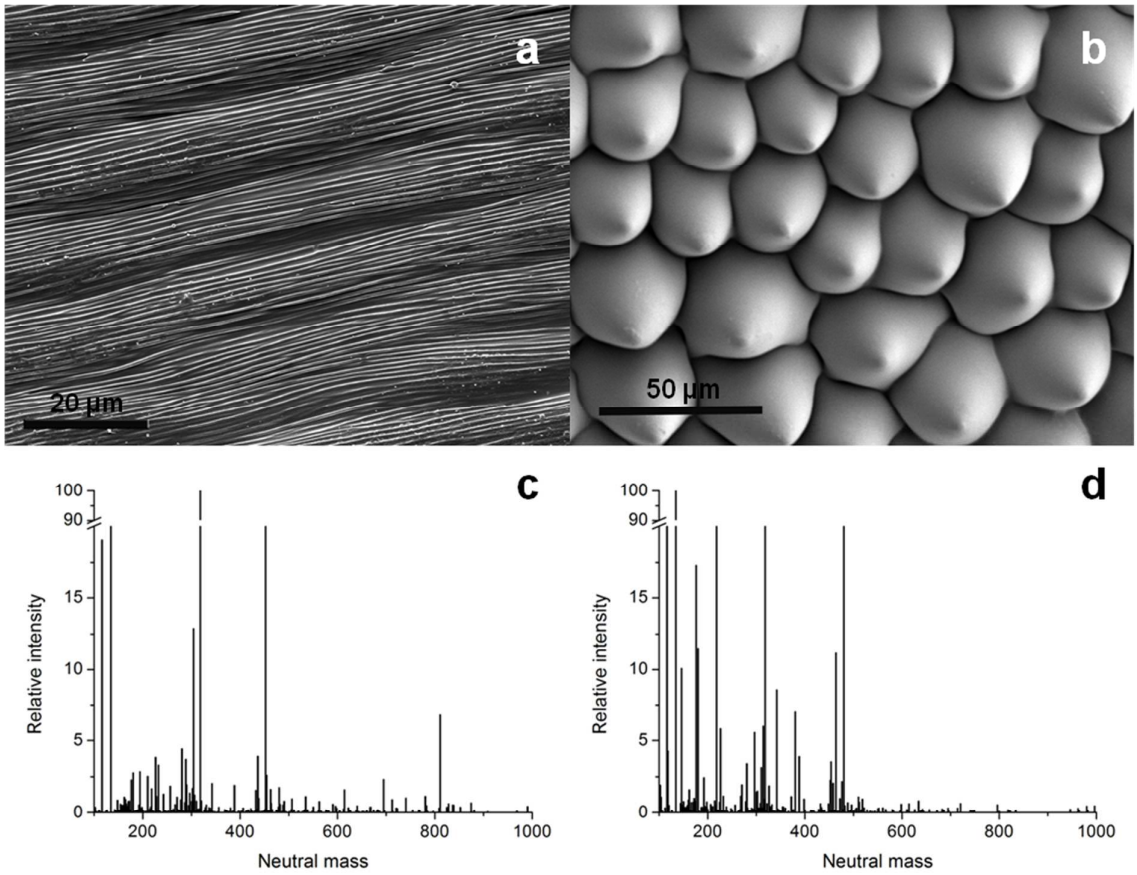

Figure 2. SEM images of the anthocyanic/ridged (a) and white/smooth (b) portions of the upper surface of a petal of *Hibiscus trionum* and corresponding mass spectra (blank subtracted and including the sum of all CHO compounds) measured using LESA-MS of the anthocyanic/ridged (c) and white/smooth (d) portions. Experimental details of SEM analysis can be found in the supporting information (section S1.4).

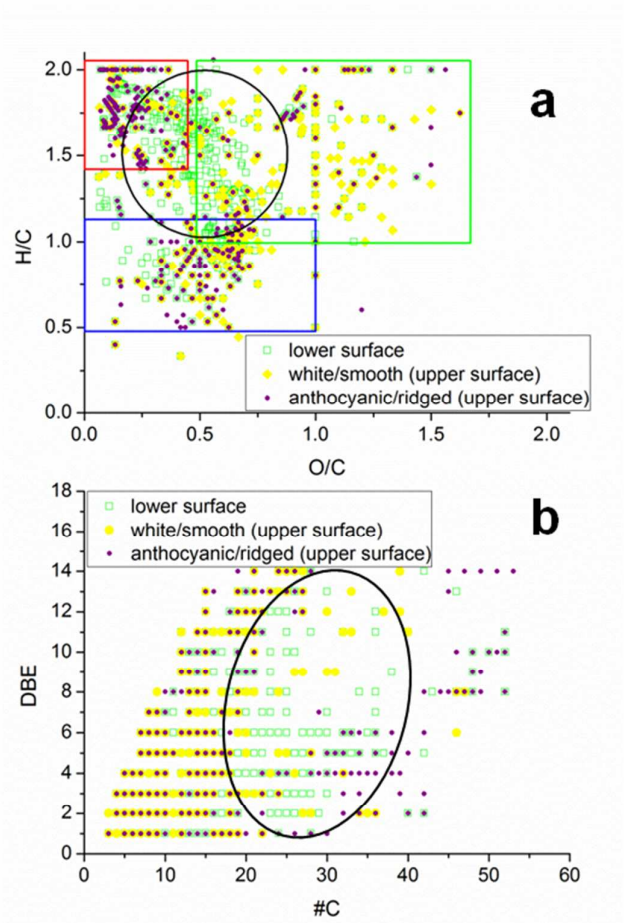

Figure 3. (a) Van Krevelen diagram showing the distribution of all compounds detected on the different portions of the petals. The red square indicates the area of lipids, the green square indicates the distribution of the majority of compounds present exclusively in the white/smooth region of the upper surface of the petal, the blue square indicates the region of unsaturated long chain compounds and the black circle indicates the majority of compounds present exclusively on the lower surface of the petals. (b) Double bond equivalents vs. number of carbons for all CHO compounds detected on the lower surface, the anthocyanic/ridged portion and the white/smooth portion on the upper surface of the petals. The black circle indicates C20-C30 polyunsaturated compounds detected on the lower surface of the petals.

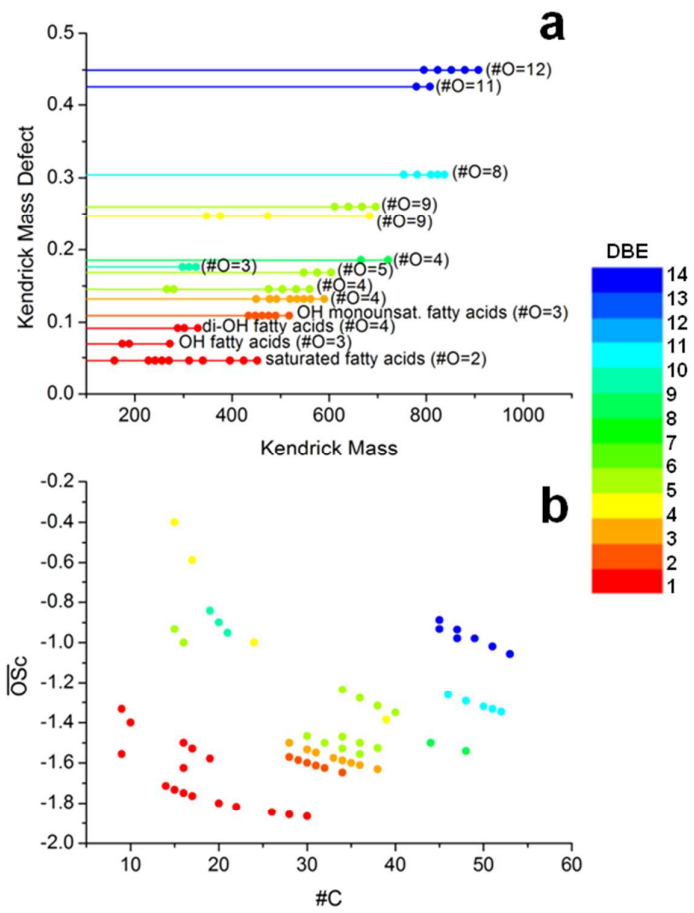

Figure 4. Kendrick mass defect plot (a) and carbon oxidation state plot (b) of the main homologous series of compounds present exclusively on the anthocyanic/ridged portion on the upper surface of the petals. Long chain highly unsaturated compounds are represented in green/blue colours (DBE>8). Number of oxygen atoms in each series of molecular formulas are reported in brackets (e.g. "#O=2").

Table 1. List of main compounds (most intense peaks in the mass spectra) detected with LESA-MS in both positive and negative ionisation in all portion of the petals on both the upper and lower surface.

Theoretical Neutral Mass	Molecular Formula	DBE	Class	Tentative Assignment[a]	MS/MS analysis[b]
116.01096	$C_4H_4O_4$	3	LMWOA[c]	Maleic acid (possible fragment)	71($C_3H_3O_2$)
134.02153	$C_4H_6O_5$	2	LMWOA	Malic Acid	115($C_4H_3O_4$)
176.03209	$C_6H_8O_6$	3	LMWOA	Ascorbic Acid	115($C_4H_3O_4$) 87($C_3H_3O_3$) 71($C_3H_3O_2$) 59($C_2H_3O_2$)
170.02153	$C_7H_6O_5$	5	LMWOA	Gallic acid	Not Done
174.01644	$C_6H_6O_6$	4	LMWOA	Dehydroascorbic acid	Not Done
192.02701	$C_6H_8O_7$	3	LMWOA	Citric acid	173($C_6H_5O_6$) 111($C_5H_3O_3$)
192.06339	$C_7H_{12}O_6$	2	LMWOA	Quinic acid	Not Done
196.05831	$C_6H_{12}O_7$	1	LMWOA	Gluconic acid	Not Done
296.07435	$C_{10}H_{16}O_{10}$	3	LMWOA	Malic acid hexoside	Not Done
146.06914	$C_5H_{10}O_3N_2$	2	Aminoacid	Glutamine	127($C_5H_7O_2N_2$) 101($C_4H_5O_3$)
162.05282	$C_6H_{10}O_5$	2	Sugar	Levoglucosan	Not Done
180.06339	$C_6H_{12}O_6$	1	Sugar	Monosaccharide[d]	161($C_6H_9O_5$) 143($C_6H_7O_4$)
342.11622	$C_{12}H_{22}O_{11}$	2	Sugar	Disaccharides[d]	179($C_6H_{11}O_6$)
256.24023	$C_{16}H_{32}O_2$	1	Fatty acid	Palmitic acid	No fragments detected
302.04265	$C_{15}H_{10}O_7$	11	Flavonoid	Quercetin/Morin	Not Done
318.03757	$C_{15}H_{10}O_8$	11	Flavonoid	Gossypetin[e] (possible fragment)	179($C_8H_3O_5$) 151($C_7H_3O_4$)
320.05322	$C_{15}H_{12}O_8$	10	Flavonoid	dihydrogossypetin	Not Done
432.10565	$C_{21}H_{20}O_{10}$	12	Flavonoid	Tannin/flavonone	Not Done
452.05910	$C_{19}H_{16}O_{13}$	12	Flavonoid	Tannin/Polyphenolic compound	317($C_{15}H_9O_8$) 289($C_{15}H_{13}O_6$) 133($C_4H_5O_5$)
464.09548	$C_{21}H_{20}O_{12}$	12	Flavonoid	Myricitrin, Isoquercetin, Spiraeoside	301($C_{15}H_9O_7$)
480.09040	$C_{21}H_{20}O_{13}$	12	Flavonoid	Myricetin-3-O-Glucoside (Tannin)/Gossypin	317($C_{15}H_9O_8$)
194.02153	$C_9H_6O_5$	7	unknown	Unknown	Not Done
232.02192	$C_8H_8O_8$	5	unknown	Unknown	Not Done

[a] Assignment made on the basis of the molecular formula (from accurate mass measurement) and MS/MS analysis where available

[b] Mass-to-charge ratios and formulas of ions measured in negative ionisation

[c] LMWOA = Low Molecular Weight Organic Acid

[d] Present as $[M-H]^-$ and $[M+Cl]^-$ in negative ionisation and $[M+H]^+$, $[M+Na]^+$, $[M+K]^+$ and $[M+NH_4]^+$ in positive ionisation

[e] Main fragments detected in this study corresponds to molecular formulas with an additional loss of –OH of the two fragments m195 and m167 detected by Braunberger et al.[54] while all other fragments were detected in both studies. In our study, the peak at mass 318.03757 could represent the superimposition of gossypetin and fragments of peaks at masses 452.05910 and 480.09040.

for TOC only

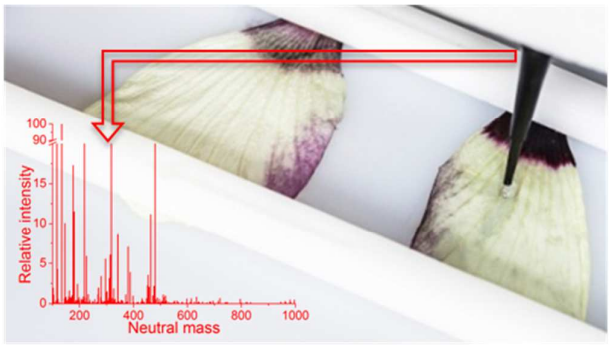
100
90
15
10
5
0
Relative intensity
200
400
600
800
1000
Neutral mass